

1
2
3
4
5
6
7
8
9
10
11
12
13
14
15
16
17
18
19
20
21
22
23
24
25
26
27
28
29
30
31
32
33
34
35
36
37
38
39
40
41
42
43
44
45
46
47
48
49
50
51
52
53
54
55
56
57
58
59
60
61
62
63
64
65

Surface tension and density of RENE N5[®] and RENE 90[®] Ni - based superalloys

Donatella Giuranno, Stefano Amore, Rada Novakovic*, Enrica Ricci

Institute for Energetics and Interphases – National Research Council (IENI-CNR),

Via de Marini 6, Genoa 16149, Italy

Donatella Giuranno, e-mail: d.giuranno@ge.ieni.cnr.it

Stefano Amore, e-mail: stefano.amore@ge.ieni.cnr.it

Enrica Ricci, e-mail: e.ricci@ge.ieni.cnr.it

* Corresponding author: Rada Novakovic

Tel. +39 –010-6475724, Fax +39 –010-6475700, e-mail: r.novakovic@ge.ieni.cnr.it

1
2
3
4 **Abstract**
5

6 The surface tension and density of Ni-based superalloys RENE N5[®] and RENE 90[®] have been
7 measured by the pinned drop method at temperatures ranging from 1638 to 1780 K. In order to
8 obtain accurate reliable data, the tests have been performed under a reducing atmosphere to
9 minimize the oxygen contamination. In the temperature ranges investigated, both properties
10 show a linear temperature dependence. With the aim of evaluating the reliability of the data, the
11 present results have been analyzed by using different thermodynamic models. The new
12 experimental data for RENE N5[®] and RENE 90[®] superalloys were also compared with the
13 corresponding data obtained by different experimental techniques.
14
15
16
17
18
19
20
21
22
23
24
25
26
27

28 **Keywords:** RENE N5[®]; RENE 90[®]; Ni-based superalloys; pinned drop method; surface tension;
29 density
30
31
32
33
34
35

36 **Introduction**
37

38 In recent years, there has been a growing interest in Ni-based superalloys came up because they
39 exhibit a peculiar combination of properties such as high strength, toughness and resistance to
40 degradation in oxidizing and corrosive environments. The presence of a Ni₃Al ordered
41 intermetallic phase in their microstructure, designated as γ' , is key to strengthening. The major
42 applications of Ni-based superalloys are for turbine turbine materials, jet and rocket engines
43 working at high temperatures and high stress levels, low-emission energy effective engines for
44 cars and aerospace as well as functional materials with high efficiency in transport using
45 electrical energy. Superalloys are also used in nuclear power and chemical processing plants, for
46 production of the so-called supermetals, i.e. amorphous metal alloys such as thin sheets for
47
48
49
50
51
52
53
54
55
56
57
58
59
60
61
62
63
64
65

1
2
3
4 electronic components with high ultimate strength to weight ratio, as construction materials for
5
6 furnace parts, for biocompatible medical implants such as hip replacements, and fine metallic
7
8 powders used to catalyze chemical reactions [1, 2]. There are many different metal casting
9
10 processes used in the manufacture of simple or complicated components. Since the casting
11
12 process involves complex interactions between various parameters related to material
13
14 composition, surrounding environments, operating conditions and steps in the process, the
15
16 manufacture of defect free casting products is almost impossible. Indeed, to reduce or, if
17
18 possible, to prevent formation of casting defects such as freckles, white spots and spurious grain
19
20 growth, much attention has been paid to the modelling of solidification. The development of
21
22 numerical optimization techniques, the availability of commercial software packages together
23
24 with a new generation of powerful supercomputers and accurate property data obtained using
25
26 advanced laboratory techniques, are needed for the design of materials through controlling
27
28 composition and microstructure, in order to optimize their final properties [3, 4]. An efficient
29
30 tool for the prediction of microstructural evolution during solidification is the phase-field
31
32 method, recently applied to Ni-based alloys [5]. This approach can be extended readily to other
33
34 grades of superalloys, such as CMSX-4[®], RENE N5[®], etc. But, the use of such mathematical and
35
36 numerical tools for the modelling of solidification is often limited by the lack or paucity of
37
38 reliable thermophysical property data, such as surface tension and density, thermal conductivity,
39
40 diffusivity and the viscosity of relevant liquid metals and alloys, needed as input parameters for
41
42 the computational models [6,7]. Among the thermophysical properties, density and surface
43
44 tension are two critical parameters for modelling fluid flow during the solidification process,
45
46 affecting both the dendrite morphology and the complex interactions between the solid and
47
48 liquid phases of the mushy zone that may lead to the formation of defects [1]. Despite the
49
50
51
52
53
54
55
56
57
58
59
60
61
62
63
64
65

1
2
3
4 importance of Ni-based alloys, a scarcity or sometimes, the lack of thermophysical property is
5
6 observed, owing to the experimental difficulties related to high temperature measurements.
7
8

9 There are different factors that hamper this type of experiments, such as high melting
10 temperatures, high chemical reactivity of many liquid alloys and the influence of gas impurities,
11 in particular on the surface properties. Among all the contaminants, oxygen plays a crucial role
12 because it strongly affects both, the surface tension and its temperature coefficient, even if it is
13 present in only trace amounts [8, 9]. This fact has been experimentally confirmed with pure
14 metals [10, 11] and their alloys [12] through the use of different measurement techniques. In
15 addition, the high reactivity of molten industrial alloys, such as Ti- and Ni-based superalloys [13,
16 14], respectively, together with difficulties in finding chemically inert or highly resistant crucible
17 or support materials in order to avoid the reactions at the interface, have to be taken into account
18 when dealing with conventional surface tension experiments.
19
20
21
22
23
24
25
26
27
28
29
30
31
32

33 In the present work, the surface tension and the density of RENE N5[®] and RENE 90[®] Ni-based
34 alloys have been measured by the pinned drop method and the new experimental results have
35 been compared with the corresponding data obtained by other techniques under both 1-g and μ -g
36 conditions in the framework of the Thermolab Project [15].
37
38
39
40
41
42
43
44
45
46

47 **Experimental procedure**

48 Sample preparation

49
50 The samples of RENE N5[®] and RENE 90[®] were taken from the same batches and used by the
51 different research groups participating in the Thermolab project [15]. Nominal compositions of
52 the two superalloys have not been provided by the manufacturers, but Energy Dispersive
53 Spectroscopy (EDS) analysis was used to determine their compositions (Table 1). A slight
54
55
56
57
58
59
60
61
62
63
64
65

1
2
3
4 difference between the compositions of RENE N5[®] determined by EDS presented in this work
5
6 and those given in other sources is found. The composition of RENE 90[®] was found to be
7
8 identical to that determined by other members of the Thermolab project, and is given in Table 1.
9

10
11 The samples were cut into small pieces with a mean mass of 2.5 g. Prior to the measurement,
12
13 each sample was mechanically abraded and chemically cleaned with organic solvents in an
14
15 ultrasonic bath. The samples were weighed before and after the experiments and losses were
16
17 observed.
18
19

20 21 22 23 24 Experimental apparatus and procedure

25
26 All the measurements were performed in an "ad hoc" designed experimental apparatus utilizing
27
28 applying a variant of the large drop method [16] called the pinned drop method [17]. A special
29
30 circular crucible with sharp edges is used in order to block the triple line at an "apparent" contact
31
32 angle leading to a value than reality, and to impose an axisymmetry on the drop. This method
33
34 allows to use larger drop than in the classic sessile drop method, and thus, a higher accuracy in
35
36 the determination of geometrical factors (e.g. diameters, surface area, height, etc.) can be
37
38 achieved [8]. The experimental apparatus and the procedure adopted have been detailed in
39
40 previous works [18, 19]. The temperature of the samples was measured using a calibrated Pt/Pt-
41
42 10%Rh thermocouple placed close to the sample. During the surface tension measurements, the
43
44 temperature of the sample was found to be stable within ± 2 K. Following cleaning, the sample
45
46 was placed in a non-oriented monocrystalline alumina (sapphire) crucible ($r = 5.5$ mm) which
47
48 was placed on the sliding alumina holder of the experimental apparatus. When the apparatus
49
50 experimental conditions (temperature, oxygen partial pressure) had been reached, the sample was
51
52 introduced into the center of the furnace with the aid of a magnetic manipulator. The surface
53
54
55
56
57
58
59
60
61
62
63
64
65

1
2
3
4 **tension and density measurements** of RENE N5[®] and RENE 90[®] Ni-based superalloys **were**
5
6 carried out at temperatures ranging from their melting point to 1780 K under a reducing flowing
7
8 atmosphere (Ar-5 at% H₂ mixture; mean flow rate $q = 0.8 \cdot 10^{-6} \text{ m}^3 \cdot \text{s}^{-1}$). The oxygen partial
9
10 pressure, P_{O₂}, was monitored by using two ZrO₂ oxygen sensors (μ -gauges POAS/SETNAG[®])
11
12 with the Pd/PdO as internal reference. The sensors measure the oxygen content in the feed and in
13
14 the exhaust gas, giving a value around P_{O₂} = 10⁻¹⁸ Pa at 973 K. In order to further reduce the
15
16 oxygen content, close to the alloy sample a Zr foil acting as an oxygen getter has been placed.
17
18
19 The temperature was decreased step by step from 1780 K to the corresponding melting points of
20
21 1641 and 1658 K for RENE 90[®] and RENE N5[®] [20], respectively. At each temperature, the
22
23 sample was allowed to equilibrate for a time ranging from 10 to 20 min. The profile of the liquid
24
25 drop was acquired using a CCD camera **operating** for a time between 10 and 15 min. **The image**
26
27 **acquisition frequency was up to 10 images per second.** The surface tension was calculated by
28
29 using a nonlinear regression method developed by Maze and Burnet [21]. The images were
30
31 processed with a dedicated acquisition software in a LABView[®] environment which **allowed** the
32
33 elaboration of surface tension and other drop parameters in real time [17, 18]. The density values
34
35 were obtained from the ratio of the drop weight and the measured volume at each temperature
36
37 **step** during the pinned drop experiments. The experimental values **presented** are results **from**
38
39 different measurement runs. **By consideration of** the experimental uncertainties **involved**, the
40
41 total error in the surface tension and density values is estimated to be about ± 3 %. After each
42
43 experiment the samples **were** further analyzed **using** SEM-EDS in order to check the surface
44
45 conditions of the solidified drop and any **changes** in the final composition.
46
47
48
49
50
51
52
53
54
55
56
57
58

59 **Results and discussion**

60
61
62
63
64
65

1
2
3
4 Some information on the thermophysical and mechanical properties of RENE N5[®] superalloy are
5 already known [2,4,20,22-24], while in relation to RENE 90[®] there are only a few
6 thermophysical property data available [20], and these have been obtained in the framework of
7 the Thermolab Project [15]. However, discrepancies in the reported data, such as the composition
8 of RENE N5[®], listed in Table 1 [2,4,20,22-24], and as a consequence, different liquidus and
9 solidus temperatures [2,20,22,24] as well as different values of other alloy properties can be
10 observed [2, 4]. To our knowledge, there is only one paper related to the surface tension and
11 density studies of liquid RENE N5[®] and RENE 90[®] [20]. In the present work the liquidus
12 temperatures of RENE N5[®] and RENE 90[®] superalloys, $T_m = (1658 \pm 11)$ K and $T_m = (1641 \pm$
13 $10)$ K [20], respectively, are the results of the Thermolab Project [15], and these values are used
14 as reference data in the equations describing the temperature dependence of their surface tension
15 and density. It is worth noting that during the surface tension measurements performed on RENE
16 N5[®] alloy, the sample appeared to be in the liquid phase even at a temperature of 20 K below its
17 melting point; as has been observed in other industrial Ni-based alloys, such as CMSX-4[®],
18 CMSX10[®] and CM186LC[®] [25].

19
20
21
22
23
24
25
26
27
28
29
30
31
32
33
34
35
36
37
38
39
40
41 The thermodynamic analysis presented here has been undertaken in order to evaluate the validity
42 and reliability of the data sets obtained. The new experimental data have been analyzed with
43 respect to the binary and ternary subsystems by using different thermodynamic models and
44 comparing to the corresponding data reported in [20]. A similar analysis has been reported for
45 CMSX-4[®] superalloy [18], Al-Nb-Ti and Al-Ta-Ti alloys [13].

46
47
48
49
50
51
52
53
54
55
56 Surface tension
57
58
59
60
61
62
63
64
65

1
2
3
4 The surface tension of RENE N5[®] and RENE 90[®] (Table 1) has been measured from their
5
6 melting point to 1780 K. For the superalloys investigated, the surface tension data obtained under
7
8 the conditions described above, obey a linear relationship. The new surface tension values of the
9
10 two superalloys are shown in Figs. 1 and 2, respectively. Each measured value shows a deviation
11
12 of about $\pm 25 \text{ mN} \cdot \text{m}^{-1}$ around the mean value. The temperature dependence of the surface
13
14 tension of RENE N5[®] and RENE 90[®] is described by Eqs. (1) and (2), respectively.
15
16
17
18
19
20

$$\gamma_{RENE N5} / \text{mN} \cdot \text{m}^{-1} = 1752 - 0.67 \cdot (\text{T/K} - 1658) \quad (1)$$

$$\gamma_{RENE 90} / \text{mN} \cdot \text{m}^{-1} = 1851 - 0.52 \cdot (\text{T/K} - 1641) \quad (2)$$

21
22
23
24
25
26
27
28
29
30 For both Ni-based superalloys investigated the surface tension decreases with increasing
31
32 temperature. Taking into account that the Al content of RENE N5[®] is almost double that of
33
34 RENE 90[®] (Table 1) and the surface tension values are significantly lower, the surface tension
35
36 polytherms of RENE N5[®] and RENE 90[®] are consistent with each other and are shown in Figs. 1
37
38 and 2, respectively, together with the corresponding literature data [20]. Until now, the surface
39
40 tension data of liquid RENE N5[®] (Fig. 1) are only data set available in the literature and thus, a
41
42 comparison is not possible.
43
44
45
46
47
48

49 <Fig. 1>
50
51
52
53

54 The surface tension temperature coefficients of the RENE N5[®] polytherm, i.e. $d\gamma/dT = -0.67$
55
56 $\text{mN} \cdot \text{m}^{-1} \cdot \text{K}^{-1}$ is obtained by linear regression fitting (Eq. (1)) and the experimental points agree
57
58 with the corresponding calculated values within the uncertainty of the measurement method.
59
60
61
62
63
64
65

1
2
3
4 The new surface tension values of the liquid RENE 90[®] alloy obtained in the present work are
5
6 higher than those reported in the literature [20] and compared with data measured using the
7
8 oscillating drop method in ground based electromagnetic levitation (EML-OD) and during the
9
10 parabolic flights experiments (PF-OD), they exhibit a maximum difference of 7 and 11%,
11
12 respectively. In particular, the slopes of the surface tension polytherms are significantly different,
13
14 as shown in Fig. 2.
15
16
17
18
19
20

21 <Fig. 2>
22
23
24
25

26 The literature data on the surface tension of liquid RENE 90[®] alloy [20] agree with each other
27
28 within an experimental error of about 4 %. The data obtained by PF-OD and by EML-OD exhibit
29
30 a good agreement close to the liquidus temperature, while with an increase in temperature a
31
32 greater difference between the two data sets can be observed because the temperature
33
34 coefficients are significantly different. In fact, as shown in Fig. 2, the surface tension polytherms
35
36 have negative slopes, i.e. $d\gamma/dT_{PF-OD}$ takes values of -0.425 and -0.447, while $d\gamma/dT_{EML-OD}$ is -
37
38 0.216 $mN \cdot m^{-1} \cdot K^{-1}$, a difference of 100%.
39
40
41
42
43

44 As already mentioned above, the RENE N5[®] and RENE 90[®] alloy samples from the same batch
45
46 have been used for surface tension measurement by different experimental methods and thus, in
47
48 all cases, the alloy compositions and the levels of impurities should have no influence on the
49
50 scatter in the results observed. Therefore, the discrepancies between the experimental results
51
52 measured by the pinned drop method and the two data sets obtained by the PF-OD and EML-OD
53
54 containerless methods probably arise from differing amounts of oxygen present in the working
55
56 atmospheres as well as from the determination of experimental temperature. A modification of
57
58
59
60
61
62
63
64
65

1
2
3
4 the sample composition as a result of oxidation may have had an influence on the previous
5
6 measurements. In addition, concerning the OD methods, the elaboration of the oscillating spectra
7
8 of complex Ni-based superalloys may also be a critical point in the determination of the surface
9
10 tension values. SEM-EDS analysis performed on RENE N5[®] and RENE 90[®] superalloys
11
12 revealed the presence of highly reactive elements, such as Al, Re, Ta and Ti, which have great
13
14 influence on the surface tension values owing to their intrinsic reactivity in a gaseous
15
16 environment as well as with common crucible materials. The surface tension of metallic melts,
17
18 such as Ni-based superalloys containing various reactive metals (Table 1) can be strongly
19
20 affected by certain surface-active elements, mainly oxygen or/and sulphur. Even trace amounts
21
22 of these surfactants can drastically reduce the surface tension of these alloys and affect the
23
24 reliability of the experimental data [9]. Therefore, further analysis of the surface tension values
25
26 obtained for RENE N5[®] and RENE 90[®] has been undertaken in order to evaluate the validity and
27
28 reliability of the two data sets.
29
30
31
32
33
34

35
36 In the case of complex alloys it is possible to estimate a property value analyzing a key binary
37
38 and/or ternary subsystem formed by the major components of a multicomponent system of
39
40 interest and taking into account the effects of the minority components on that property. Ni, Al
41
42 and Cr are the major alloying elements in both RENE N5[®] and RENE 90[®] alloys (Table 1) and
43
44 hence the surface tension values of two Ni-based superalloys were compared to the model based
45
46 predictions for Al-Ni and Al-Cr-Ni liquid alloys as well as to the data reported in [20].
47
48
49
50 Mathematical formalisms of thermodynamic models used in the present work to calculate the
51
52 surface tension of liquid binary and ternary alloys have been described in detail in our previous
53
54 papers [9,13]. The thermodynamic data and the optimized data set of the excess Gibbs free
55
56 energy of mixing of liquid Al-Ni [26], Al-Cr, Cr-Ni and Al-Cr-Ni alloys [27], the melting
57
58
59
60
61
62
63
64
65

1
2
3
4 temperatures, densities and molar volumes of pure components [28] as well as the surface
5
6 tension reference data of Al [29], Cr [30] and Ni [31] were taken as input data for the
7
8 calculations of the surface tension isotherms and iso-surface tension lines. It is important to
9
10 mention that reliable input data **must** be chosen in order to reduce **any disparity** between the
11
12 predicted and experimental values.
13
14

15
16 The surface tension of Al-Ni liquid alloys **has** been investigated by the perfect solution model, by
17
18 the Quasi-Chemical Approximation (QCA) for the regular solutions [32] and by the Compound
19
20 Formation Model (CFM) [33], a simple structural model for the chemical complexes. The AlNi
21
22 intermediate phase was postulated as energetically favored and **thus** preferential arrangements of
23
24 Al and Ni constituent atoms favor the formation of AlNi complexes in the liquid phase. The
25
26 presence of short range order ordering in the liquid phase increases the surface tension of Al-Ni
27
28 alloys and its variations can be estimated by the difference between the surface tension isotherms
29
30 calculated by the two models. The **experimental surface tension** data of RENE N5[®] and RENE
31
32 90[®] with 14.63 and 7.46 at% Al (Table 1) are compared to the corresponding values of the
33
34 Al_{14.63}Ni_{85.37} and Al_{7.46}Ni_{92.54} **compositions**, respectively, having the same Al content **and**
35
36 **obtained using the same experimental apparatus**. The effects of the minority alloying elements on
37
38 the surface tension of Ni-based alloys are comparable, at least **to** a first approximation, to that of
39
40 liquid nickel **itself**. **Therefore, for the calculation, the Ni content was taken as the sum of the**
41
42 **amount of Ni present plus the minority alloying elements**. The surface tension isotherms of Al-
43
44 Ni liquid alloys have been calculated using the three aforementioned models for 1773 K and
45
46 together with literature data [19] are shown in Fig. 3. **The surface tension data set for the RENE**
47
48 **90[®] superalloy [20] was also analyzed with the aim of evaluating the reliability of the new**
49
50 **experimental values**.
51
52
53
54
55
56
57
58
59
60
61
62
63
64
65

<Fig. 3>

The surface tension of the $\text{Al}_{14.63}\text{Ni}_{85.37}$ alloy calculated for 1773 K by the QCA and CFM varies between 1580 and 1742 $\text{mN}\cdot\text{m}^{-1}$, while for RENE N5[®], at the same temperature, a measured value of 1675 $\text{mN}\cdot\text{m}^{-1}$ was obtained. As already discussed, the new surface tension value of RENE N5[®] is lower than that of the $\text{Al}_{14.63}\text{Ni}_{85.37}$ alloy calculated using the CFM (Fig. 3). The surface tension value for RENE N5[®] obtained by the pinned drop method and the model based prediction agree within the uncertainty of the measurement method adopted. In the case of the RENE 90[®] superalloy, the experimental surface tension value of 1782 $\text{mN}\cdot\text{m}^{-1}$ is compared to the corresponding values of 1680 and 1785 $\text{mN}\cdot\text{m}^{-1}$ calculated for the $\text{Al}_{7.46}\text{Ni}_{92.54}$ using the QCA and CFM, respectively. The pinned drop measured value is very close to that predicted by the CFM, while the data obtained by the EML-OD and by PF-OD containerless methods [15,20] are lower (Fig. 2) and agree well with the QCA predicted value, as shown in Fig. 3. In addition, it is worth emphasizing that the measurements of surface tension of two Ni-based superalloys as well as the series of Al-Ni binary alloys [19] have been carried out by using the same experimental apparatus. The experimental surface tension values obtained for the RENE N5[®] and RENE 90[®] alloys (see Fig. 3; inside a rectangular box) are close to those of the $\text{Al}_{11.4}\text{Ni}_{88.6}$ alloy (in at %) [19] having an Al content slightly different with respect to those of the two Ni-based superalloys.

Chromium, with contents of 8.20 and 10.09 at % is the third major component after Ni and Al in RENE N5[®] and RENE 90[®] (Table 1), respectively, and thus, the surface tension of Al-Cr-Ni ternary alloys having the same Al and Cr contents as the two Ni-based superalloys investigated

1
2
3
4 can be used for comparison (Fig. 4). As mentioned in the previous analysis, the contents of the
5
6 minority alloying elements in RENE N5[®] and RENE 90[®] were replaced by that of Ni.
7
8 Combining the excess Gibbs free energies of mixing of the three binary subsystems with that of
9
10 the Al-Cr-Ni [27], the surface tension of liquid Al-Cr-Ni ternary alloys was calculated for T =
11
12 1773 K using the Butler model. Full details of the mathematical formalism are reported in [34].
13
14 The experimental values of the surface tension of RENE N5[®] and RENE 90[®], obtained at
15
16 T=1773 K are 1675 and 1782 $mN \cdot m^{-1}$, respectively, while the corresponding values calculated
17
18 for ternary Al_{14.63}Cr_{8.2}Ni_{77.17} and Al_{7.46}Cr_{10.09}Ni_{82.45} (in at %) alloys amount to 1585 and 1700
19
20 $mN \cdot m^{-1}$, respectively, as shown in Fig. 4.
21
22
23
24
25
26
27
28
29
30
31
32
33

<Fig. 4>

34 The calculated surface tension values of the Al_{14.63}Cr_{8.2}Ni_{77.17} and Al_{7.46}Cr_{10.09}Ni_{82.45} alloys are
35
36 lower (about 5 %) with respect to those of RENE N5[®] and RENE 90[®] obtained by the pinned
37
38 drop method owing to the presence of minor components having the surface tension values
39
40 higher than that of Ni. Model based predictions for different thermophysical properties of Ni-
41
42 based superalloys have been reviewed by Mills et al. [7] and, in the case of surface tension, these
43
44 authors reported probable a uncertainty of about $\pm 5\%$. Therefore, the predicted ternary values
45
46 support the new experimental surface tension data of RENE N5[®] and RENE 90[®] and can be
47
48 interpreted as a lower bound for the measured values. Bearing in mind that the surface tension
49
50 values of undercooled Cr, Co, W, Ta, Mo, Ti and Hf [10,11] are higher than those of Ni, while
51
52 the presence of surfactants, such as oxygen that, even if it is present in trace amounts, contributes
53
54 to a decrease in the surface tension of Ni-based superalloys, the corresponding values of binary
55
56
57
58
59
60
61
62
63
64
65

1
2
3
4 and ternary alloys can be useful to provide upper and lower bounds for the equilibrium surface
5
6 tension of these complex alloy systems.
7

8
9 After the surface tension measurements, each alloy sample has been analyzed by SEM-EDS and
10
11 only minor changes in composition were observed. The dendritic microstructures of RENE N5[®]
12
13 (Fig. 5a) and RENE 90[®] (Fig. 5b) Ni-based superalloys were revealed and the micrographs are
14
15 shown in Fig. 5a and 5b. Although the experimental conditions were the same, a different level
16
17 of surface oxidation on the solidified alloy drops was found (Fig. 5a and 5b).
18
19
20
21
22

23
24 <Fig. 5a and 5b>
25
26
27

28
29 Indeed, the oxygen content detected by EDS at the top surface of RENE 90[®] was lower than 0.5
30
31 at %, while in the case of RENE N5[®], it was more than 13 at %. Aluminum is one of the major
32
33 alloying elements in RENE N5[®] and RENE 90[®] having the lowest surface tension and therefore
34
35 Al atoms segregate to the surface of both superalloys. The Al content identified by SEM-EDX on
36
37 the top layers of RENE N5[®] is comparable to that detected on RENE 90[®] superalloy and,
38
39 therefore the higher initial Al content of the as received RENE N5[®] alloy (Table 1) cannot be the
40
41 only cause for its strong surface oxidation (Fig. 5a). Probably, the RENE N5[®] alloy melt may be
42
43 more susceptible to oxidation owing to the presence of highly reactive rhenium (Table 1), as it
44
45 was observed in the case of other Ni-based alloys [35].
46
47
48
49
50
51
52

53 Density

54
55 The density of the two Ni-based superalloys has been determined at the same temperatures and
56
57 by the same method used for the surface tension measurements. In order to ensure accurate
58
59
60
61
62
63
64
65

1
2
3
4 results, the experimental apparatus was calibrated using the melting point of pure gold. In the
5
6 temperature ranges investigated, the densities of liquid RENE N5[®] and RENE 90[®] decrease
7
8 linearly with increasing temperature and their temperature dependences can be described by
9

$$\rho_{RENE\ N5} / g \cdot cm^{-3} = 7.53 - 0.0016 \cdot (T/K - 1658) \quad (3)$$

$$\rho_{RENE\ 90} / g \cdot cm^{-3} = 8.01 - 0.0018 \cdot (T/K - 1641) \quad (4)$$

10
11
12
13
14
15
16
17
18
19
20
21
22 Each measured value shows a deviation of about $\pm 0.12 \text{ g} \cdot \text{cm}^{-3}$ around the mean value. The
23
24 density polytherms of RENE N5[®] and RENE 90[®] and the experimental values obtained are
25
26 shown in Figs. 5 and 6, respectively. For the alloys investigated, the density was found to
27
28 increase with decreasing Al content and the new results are congruous among them with respect
29
30 to Al content (Table 1). The measured density values of the two Ni-based superalloys are
31
32 consistently higher than those calculated by the ideal mixture approximation and the
33
34 corresponding data sets differ between 4.5 and 6.2 %, respectively. Comparable values varying
35
36 between 5 and 6 % were reported for CMSX-4[®], CMSX-10[®] and CM186LC[®] Ni-based
37
38 superalloys [25]. These findings can be substantiated by the mixing property data of liquid Al-Ni
39
40 alloys [9,19,26]. Indeed, the thermodynamic data of the Al-Ni system [26] indicate a pronounced
41
42 negative deviation from Raoult's law. From an energetic point of view, very strong exothermic
43
44 effects in this system result in tighter bonding between Al and Ni atoms and consequently a
45
46 decrease in the molar volume, leading to higher densities with respect to those of an ideal
47
48 mixture [28]. Ni-based superalloys display similar density behaviour owing to strong bonding
49
50 between Ni and Al [36] that also persists in solid solutions [2]. Mukai et al. [35] have used two
51
52 experimental methods to measure the density of liquid Ni and of a series of Ni-based alloys,
53
54
55
56
57
58
59
60
61
62
63
64
65

1
2
3
4 from binary, ternary and quaternary to complex multicomponent systems of industrial interest,
5
6 aiming to obtain reliable experimental data and subsequently to **formulate** a general prediction
7
8 model for the densities of liquid Ni-based alloys [6]. The model is based on the molar volume of
9
10 Ni and the partial molar volumes of Al, Cr, Co, W, Ta, Mo and Re, obtained from the
11
12 experimentally determined densities [35], while the molar volumes of Ti, Hf and Nb were taken
13
14 from the literature. In order to evaluate the reliability of new data sets, the Mukai model [6] has
15
16 been used to calculate the densities of RENE N5[®] and RENE 90[®] and **to compare with the**
17
18 **corresponding experimental** values. In the case of RENE N5[®], **the density data are lacking in the**
19
20 **literature** thus, it was only possible to compare the present results with the values estimated
21
22 theoretically and described by
23
24
25
26
27
28
29
30

$$\rho_{RENE\ N5}^{CALC} / g \cdot cm^{-3} = 7.54 - 0.0010 \cdot (T/K - 1658) \quad (5)$$

31
32
33
34
35
36 The measured density values are slightly lower **than those** predicted by the Mukai model [6], as
37
38 shown in Fig. 6.
39
40
41
42

43 <Fig. 6>
44
45
46
47

48 The differences between the two data sets vary from 0.3 to 1.35 % **increasing with increasing**
49
50 **temperature**, from the alloy melting point to the end of the temperature interval of measurements.
51
52

53 The discrepancies observed can be attributed to **the** different temperature coefficients of two
54
55 density polytherms (Eqs.(3) and (5)). Preliminary analysis of density data of different Ni-based
56
57 alloys indicates discrepancies between the predicted and measured values that lie within ± 2.5 %
58
59
60
61
62
63
64
65

1
2
3
4 [6,7]. The measured density values of liquid RENE 90[®] alloy are lower than those obtained by
5
6 the EML-OD [15,20] and exhibit a maximum difference of 6 %. Larger differences, of up to 8 %
7
8 were observed with respect to the corresponding predicted values [6], as it is shown in Fig. 7.
9

10
11
12
13
14 <Fig. 7>

15
16 Negative temperature coefficients of -0.00180 (Eq. (4)) and -0.00114 $g \cdot cm^{-3} \cdot K^{-1}$ [20],
17
18 respectively, agree well with each other and are comparable to that obtained by Eq. (6). The
19
20 density of RENE 90[®] predicted by the Mukai model [6] is given by
21
22

$$\rho_{RENE90}^{CALC} / g \cdot cm^{-3} = 8.49 - 0.0013 \cdot (T/K - 1641) \quad (6)$$

23
24
25
26
27
28
29
30
31

32 As shown in Fig. (7), the density values calculated by Eq. (6) are higher than the present
33
34 experimental data as well as with respect to literature data [20].
35

36 The experimental density data of RENE N5[®] and RENE 90[®] measured under the aforementioned
37
38 experimental conditions can be considered as reliable and Eqs. (3) and (4) are given as the
39
40 recommended equations for the two Ni-based superalloys investigated.
41
42
43
44
45

46 **Conclusions**

47
48 The surface tension and density of liquid RENE N5[®] and RENE 90[®] liquid Ni-based superalloys
49
50 have been measured by the pinned drop method in the temperature range from their melting
51
52 temperatures up to 1780 K. In order to evaluate the reliability of the new experimental values the
53
54 obtained property data sets have been analyzed within various theoretical frameworks and
55
56 compared with the available literature data. Model based predictions of the surface tension and
57
58
59
60
61
62
63
64
65

1
2
3
4 density of the two Ni-based superalloys exhibit a good agreement with the new experimental
5
6 data. Taking into account the different measurement methods used, the surface tension and the
7
8 density results obtained in the present work are consistent with the corresponding data sets
9
10 measured by the other research groups participating in the Thermolab project.
11
12
13
14
15

16 Acknowledgments

17
18 The authors gratefully acknowledged the ESA MAP-Thermolab Project for financial support and
19
20 Thermolab team for the helpful discussions.
21
22
23
24
25
26

27 Figure Captions

28
29 **Fig. 1** Temperature dependence of the surface tension of the liquid RENE N5[®] superalloy
30 together with the experimental data (●) from the present work.
31
32

33
34 **Fig. 2** Temperature dependence of the surface tension for the liquid RENE 90[®] superalloy
35 together with the experimental data (▲) from the present work. Literature data (-----) obtained
36 by PF-OD (curves 1a and 1b) [20] and by EML-OD (-----)(curve 2) [20] are given for
37 comparison
38

39
40 **Fig. 3** The new surface tension experimental data of liquid RENE N5[®] (▲) and RENE 90[®] (●)
41 obtained at 1773 K, together with literature data on RENE 90[®] (□) [20], (+) [20], (★) [20]. For
42 comparison, literature data on Al-Ni liquid alloys (■)[19] and the surface tension isotherms
43 calculated by: the CFM (curve 1), the QCA for the regular solution (curve 2) and the perfect
44 solution model (curve 3) are also shown
45
46

47
48 **Fig. 4** Iso-surface tension lines for liquid Al-Cr-Ni alloys calculated by the Butler model for T =
49 1773 K. The symbols (▲,●) indicate the Al_{14.63}Cr_{8.2}Ni_{77.17} and Al_{7.46}Cr_{10.09}Ni_{82.45} alloys used for
50 the evaluation of validity and reliability of new surface tension data of RENE N5[®] and RENE
51 90[®] Ni-based superalloys, respectively
52

53
54 **Fig. 5** SEM micrographs and EDS analysis of the top surface of a) RENE N5[®] and b) RENE 90[®]
55 solidified alloy drops after the pinned drop experiments performed under a reducing atmosphere
56 of Ar-5 % H₂ (in at %) mixture
57
58
59
60
61
62
63
64
65

1
2
3
4
5
6
7
8
9
10
11
12
13
14
15
16
17
18
19
20
21
22
23
24
25
26
27
28
29
30
31
32
33
34
35
36
37
38
39
40
41
42
43
44
45
46
47
48
49
50
51
52
53
54
55
56
57
58
59
60
61
62
63
64
65

Fig. 6 Temperature dependence of the density for the liquid RENE N5[®] superalloy together with the experimental data (●) of the present work. The density values calculated by the Mukai model [6] (-----) are given for comparison

Fig. 7 Temperature dependence of the density for the liquid RENE90[®] superalloy together with the experimental data (▲) of the present work and the literature data (■) obtained by EML-OD [20]. The density values calculated by the Mukai model [6] (-----) are given for comparison

1
2
3
4 **References**
5
6

- 7 1. Rappaz M and Rettenmayr M (1998) Simulation of solidification. *Current Opinion in Solid*
8 *State and Mater Sci* 3:275-282.
9
10 2. Pollock TM and Tin S (2006) Nickel-based superalloys for advanced turbine engines:
11 chemistry, microstructure, and properties. *J Propul Power* 22(2):361-374.
12
13 3. Van Sluytman JS and Pollock TM (2012) Optimal precipitate shapes in nickel-base
14 $\gamma - \gamma'$ alloys. *Acta Mater* 60:1771-1783.
15
16 4. Reed RC, Tao T, Warnken N (2009) Alloys-by-design: application to nickel-based single
17 crystal superalloys. *Acta Mater* 57:5898-5913.
18
19 5. Warnken N, Mab D, Drevermann A, Reed RC, Fries SG, Steinbach I (2009) Phase-field
20 modelling of as-cast microstructure evolution in nickel-based superalloys. *Acta Mater* 57:
21 5862-5875.
22
23 6. Mukai K, Li Z, Mills KC (2005) Prediction of the densities of liquid Ni-based superalloys.
24 *Metall Mater Trans* 36B:255-262.
25
26 7. Mills KC, Youssef YM, Li Z, Su Y (2006) Calculation of thermophysical properties of Ni-
27 based superalloys. *ISIJ Int* 46(5):623-632.
28
29 8. Brooks R, Egry I, Ricci E, Seetharaman S, Wunderlich R (2006) Thermophysical property
30 measurements of high-temperature liquid metallic alloys—state of the art. *High Temp Mater*
31 *Process* 25:303-322.
32
33 9. Egry I, Ricci E, Novakovic R, Ozawa S (2010) Surface tension of liquid metals and alloys -
34 Recent developments. *Adv Colloid Interface Sci* 159:198-212.
35
36 10. Keene BJ (1993) Review of data for the surface tension of pure metals. *Int Mater Rev* 38:
37 157-192.
38
39 11. Mills KC and Su YC (2006) Review of surface tension data for metallic elements and alloys:
40 Part 1 - Pure metals. *Int Mater Rev* 51:329-351.
41
42 12. Keene BJ (1993) The surface tension of tin and its alloys with particular reference to solders.
43 National Physical Laboratory, Teddington.
44
45 13. Nowak R, Lanata T, Sobczak N, Ricci E, Giuranno D, Novakovic R, Holland-Moritz D, Egry
46 I (2010) Surface tension of γ -TiAl-based alloys. *J Mater Sci* 45:1993-2001.
47
48 14. Sikka VK, Deevi SC, Viswanathan S, Swindeman RW, Santella ML (2000) Advances in
49 processing of Ni₃Al-based intermetallics and applications. *Intermetallics* 8:1329-1337.
50
51
52
53
54
55
56
57
58
59
60
61
62
63
64
65

-
15. Fecht HJ, Wunderlich R, Battezzati L, Egry I, Étay J, Ricci E, Seetharaman S (2008) Thermophysical Properties of Liquid Metallic Alloys. Final Report Phase II Thermolab ESA-MAP Project AO-99-022.
 16. Naidich JuV (1981) The wettability of solids by liquid metals. In: Cadenhead DA and Danielli JF (eds) Progress in Surface and Membrane Science. Academic Press, New York, pp. 353-484.
 17. Ricci E, Arato E, Passerone A, Costa P (2005) Oxygen tensioactivity on liquid-metal drops. Adv Colloid Interface Sci 117:15-32.
 18. Ricci E, Giuranno D, Novakovic R, Matsushita T, Seetharaman S, Brooks R, Chapman L, Queded P (2007) Density, surface tension, and viscosity of CMSX-4® superalloy. Int J Thermophysics 28:1304-1321.
 19. Giuranno D, Tuissi A, Novakovic R, Ricci E (2010) Surface tension and density of Al-Ni Alloys. J Chem Eng Data 55:3024-3028.
 20. Battezzati L and Baldissin D (2008) The ThermoLab Project: Thermophysical properties of superalloys. High Temp Mater and Process 27(6):423-428.
 21. Maze C and Burnet G (1971) Modifications of a non-linear regression technique used to calculate surface tension from sessile drops. Surf Sci 24:335-342.
 22. Wu RI and Perepezko JH (2000) Liquidus temperature determination in multicomponent alloys by thermal analysis. Metall and Mater Trans 31A:497-501.
 23. Campbell CE, Boettinger WJ, Hansen T, Merewether P, Mueller BA (2005) Examination of multicomponent diffusion between two Ni-base superalloys. In Turchi PEA, Gonis A, Rajan K, Meike A (eds) Complex Inorganic Solids: Structural, Stability, and Magnetic Properties of Alloys, Springer, New York, pp. 241-250.
 24. Barabash OM, Barabash RI, David SA, Ice GE (2006) Residual stresses, thermomechanical behavior and interfaces in the weld joint. Adv Eng Mater 8(3):202-205.
 25. Li Z, Mills KC, McLean M, Mukai K (2005) Measurement of the density and surface tension of Ni-based superalloys in the liquid and mushy states. Metall and Mater Trans 36B:247-254.
 26. Ansara I, Dupin N, Lukas HL, Sundman B (1997) Thermodynamic assessment of the Al-Ni system. J. Alloys Compd 247:20-30.
 27. Dupin N, Ansara I, Sundman B (2001) Thermodynamic re-assessment of the ternary system Al-Cr-Ni. Calphad 25(2):279-298.

-
28. Iida T and Guthrie RIL (1993) *The physical properties of liquid metals* 1st edn. Clarendon Press, Oxford.
 29. Lang G, Laly P, Joud JC, Desré P (1977) Measurement of the surface tension of some fluid metals by different methods. *Z Metallkd* 68:113-116.
 30. Levin ES and Ayushina GD (1971) *Russ J Phys Chem* 45(6):792-795.
 31. Naidich YuV, Perevertailo VM, Nevodnik GM (1972) Surface properties of Ni-C and Co-C melts. *Izv Russ Akad Nauk Ser Metal*:2: 22-30.
 32. Novakovic R (2011) Bulk and surface properties of liquid Al-Cr and Cr-Ni alloys. *J Phys: Condens Matter* 23:235107(1-8).
 33. Novakovic R and Tanaka T (2006) Bulk and surface properties of Al-Co and Co-Ni liquid alloys. *Physica B* 371:223-231.
 34. Plevachuk Y, Sklyarchuk V, Gerbeth G, Eckert S, Novakovic R (2011) Surface tension and density of liquid Bi-Pb, Bi-Sn and Bi-Pb-Sn eutectic alloys. *Surf. Sci.* 605:1034-1042.
 35. Mukai K; Li Z, Fang L (2004) Measurement of the densities of nickel-based ternary, quaternary and Commercial Alloys. *Mater Trans* 45(10):2987-2993.
 36. Mills KC, Youssef YM, Li Z (2006) The effect of aluminium content on thermophysical properties of Ni-based superalloys. *ISIJ Int* 46(1):50-57.

Figure1
[Click here to download high resolution image](#)

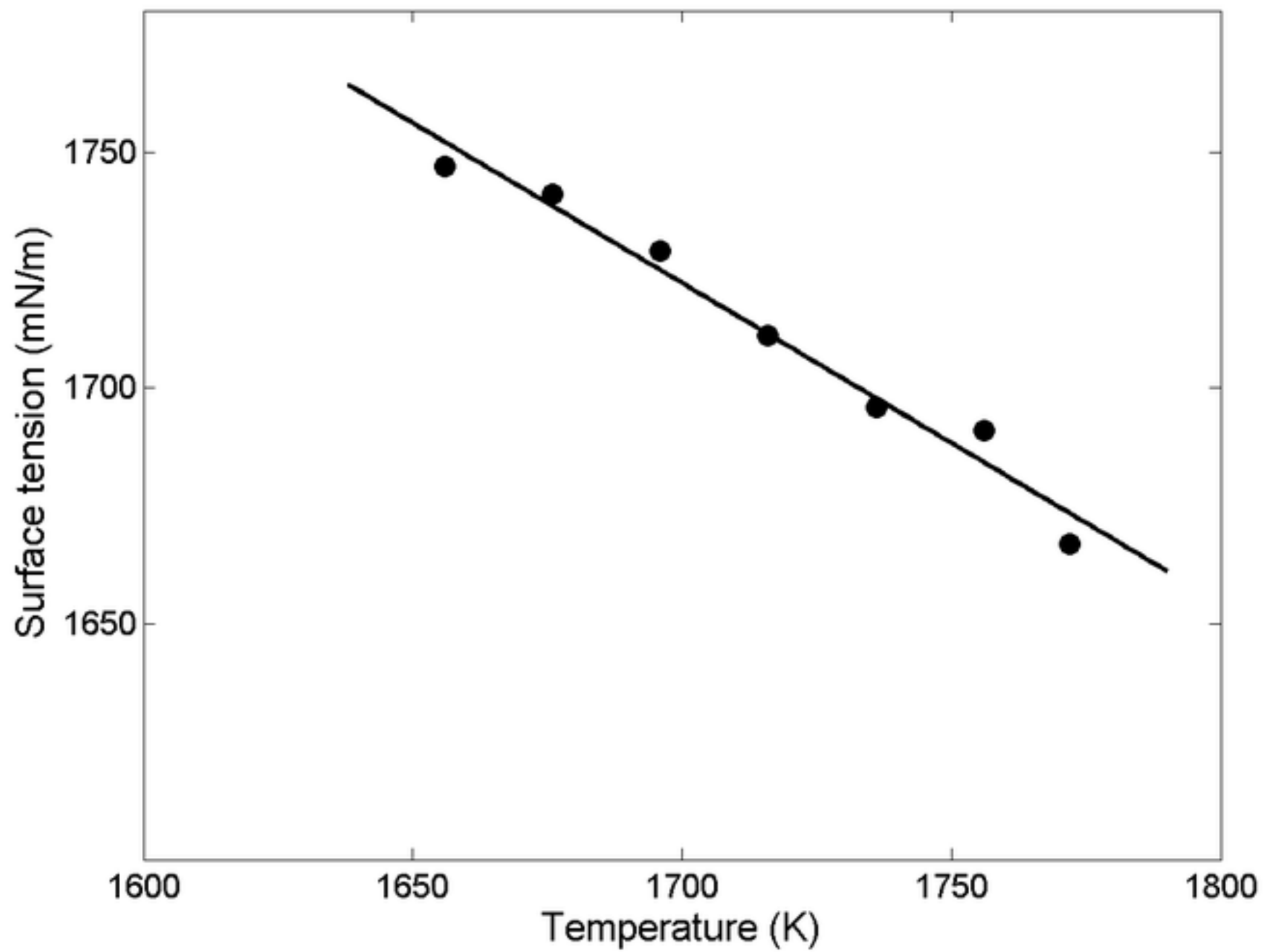


Figure2
[Click here to download high resolution image](#)

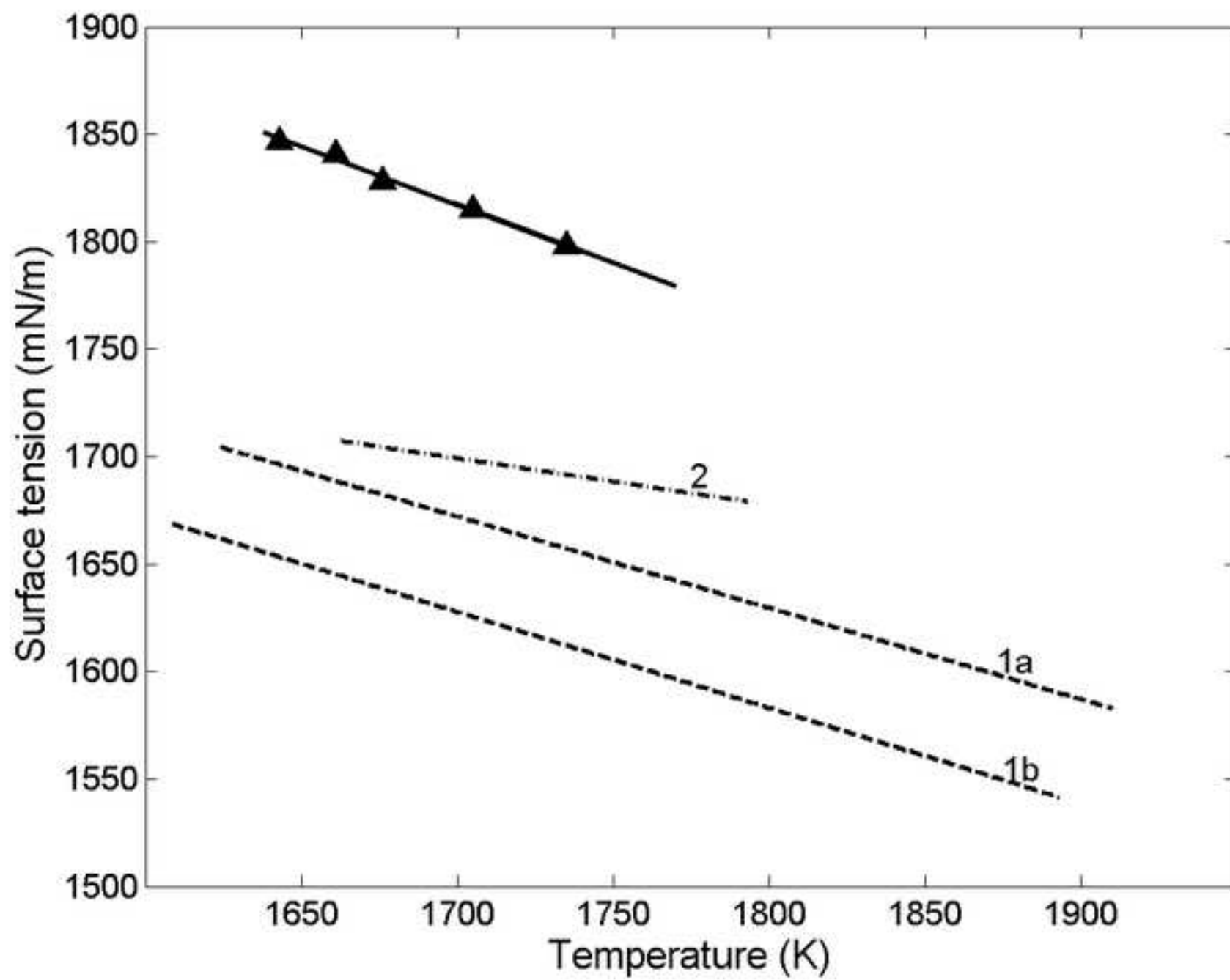


Figure3
[Click here to download high resolution image](#)

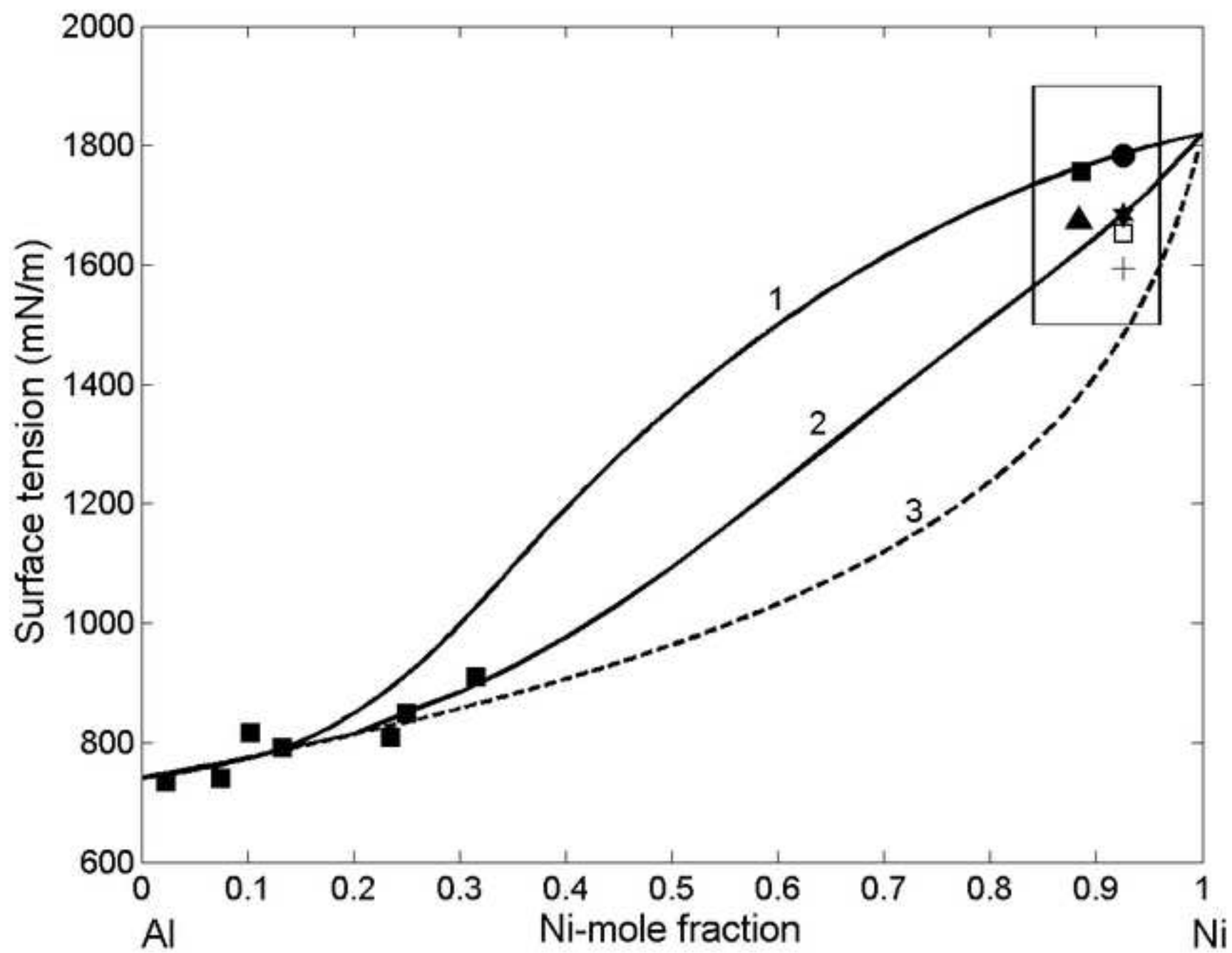


Figure4
[Click here to download high resolution image](#)

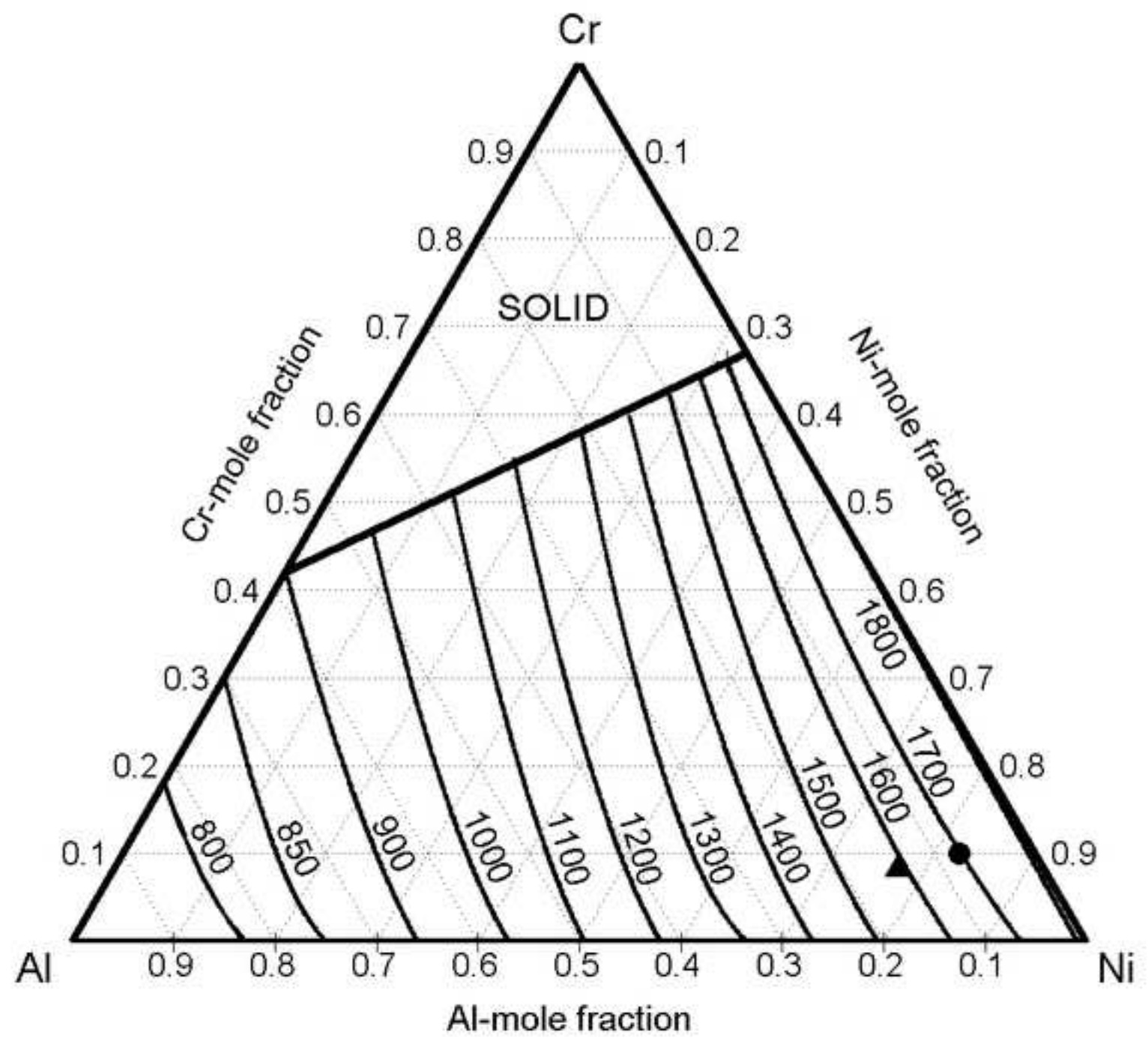


Figure5a
[Click here to download high resolution image](#)

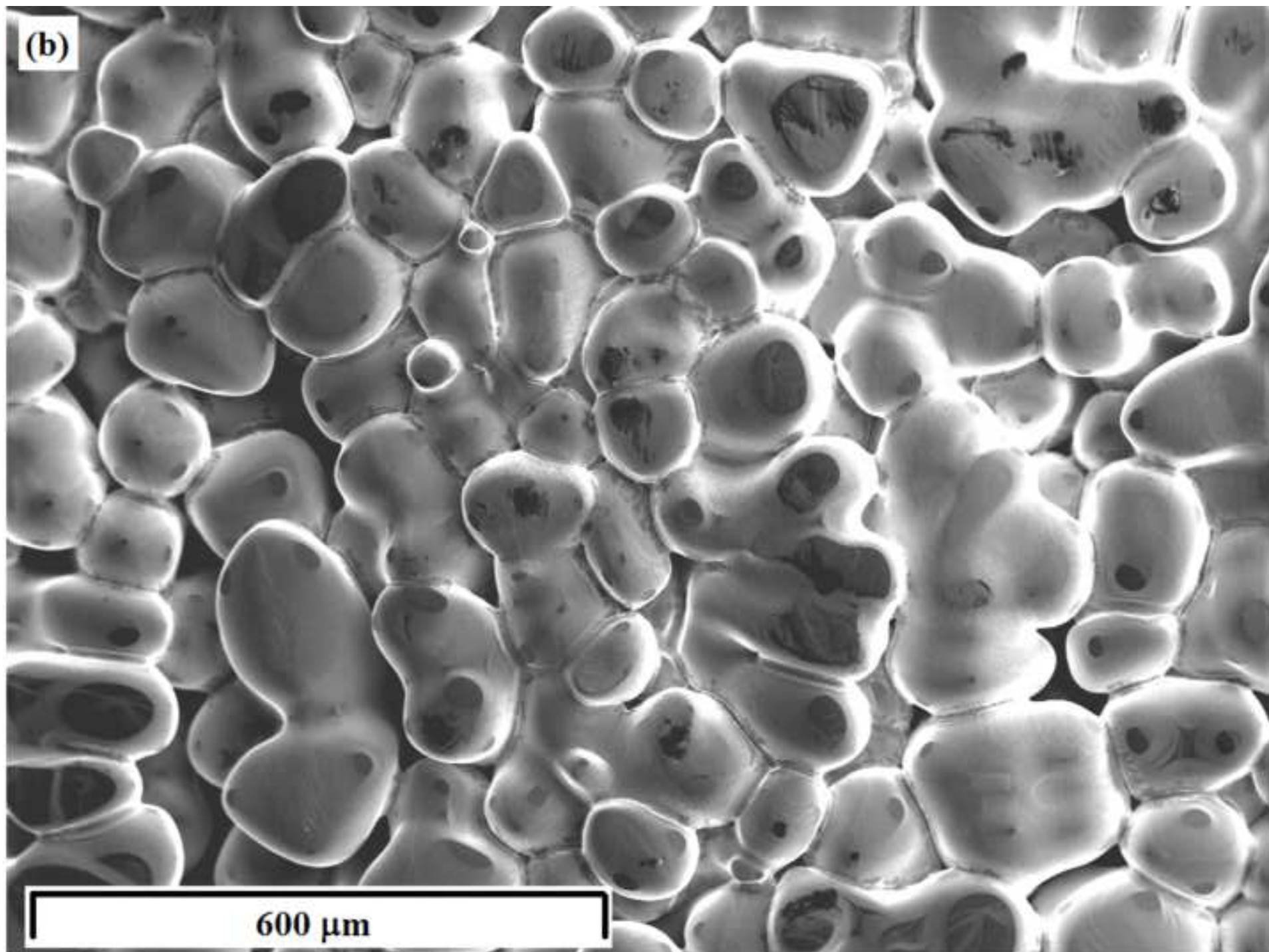


Figure5b
[Click here to download high resolution image](#)

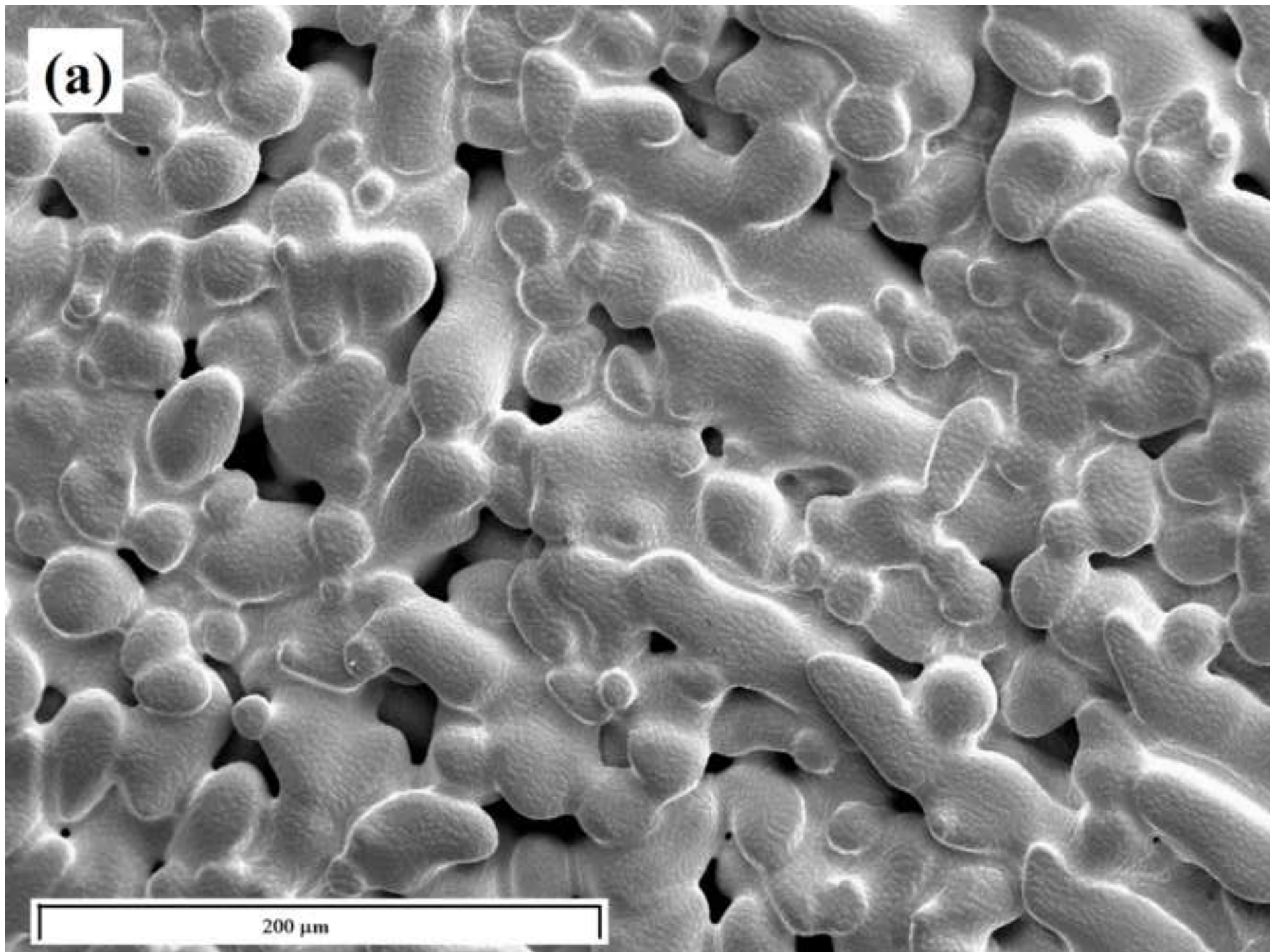


Figure6
[Click here to download high resolution image](#)

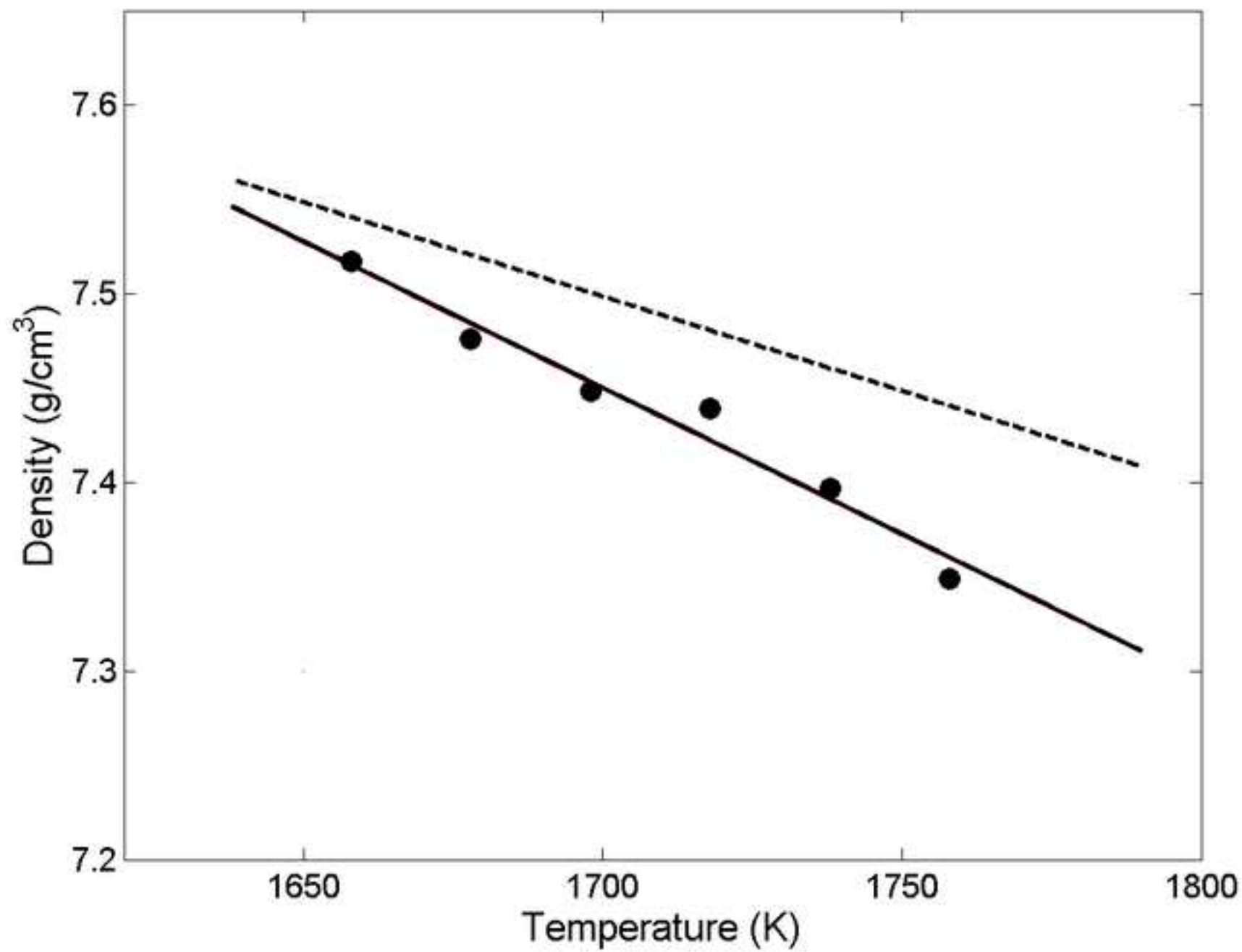


Figure7
[Click here to download high resolution image](#)

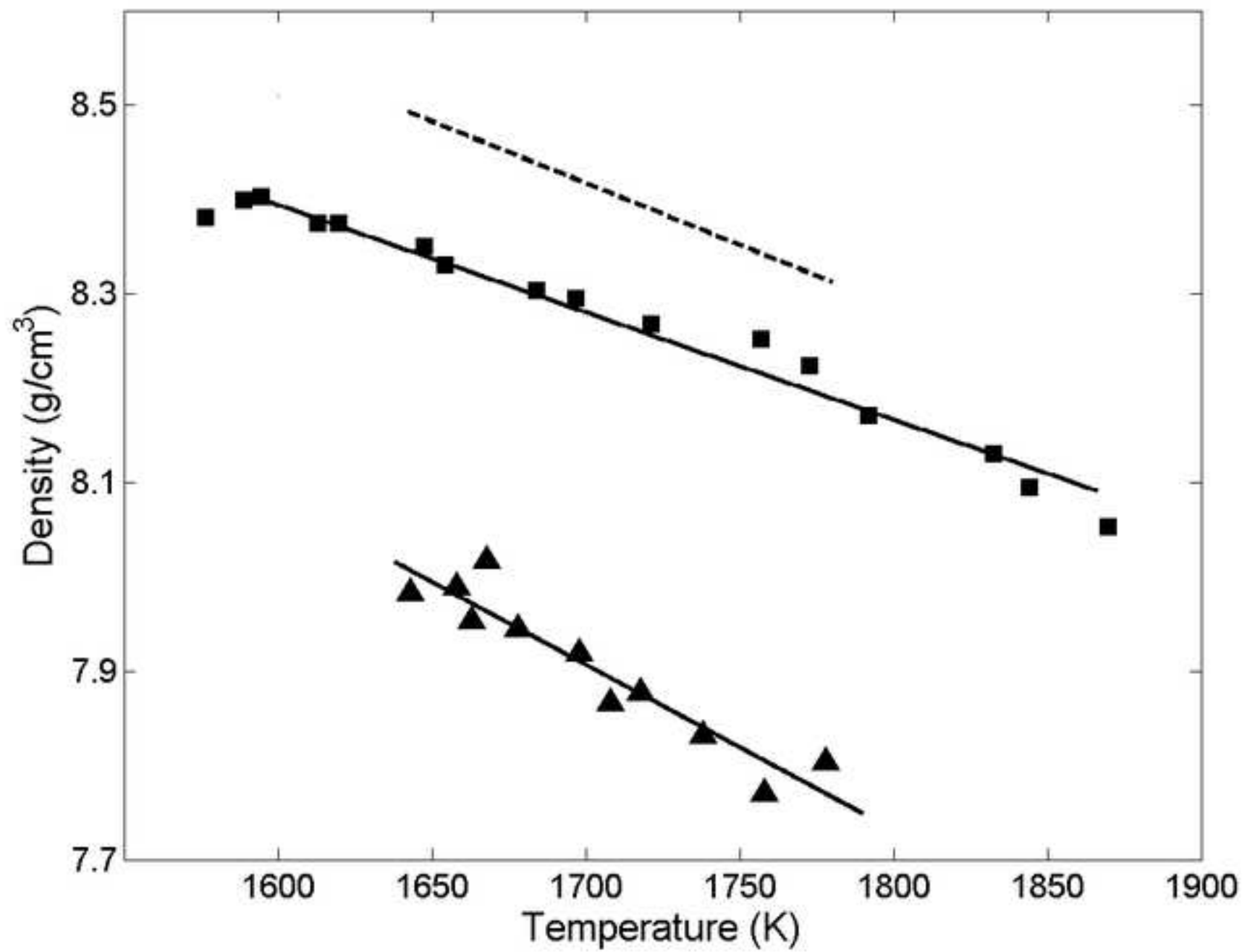


Table 1. Composition of RENE N5[®] and RENE 90[®] Ni-based superalloys^a (in wt %). The data obtained by EDS analysis are indicated by "*"

Alloy / Refs.	Ni	Cr	Co	Al	W	Ta	Mo	Ti	Re	Si	C	Nb	Hf	Y	B	Liquidus temp. / K
*RENE N5 [®] present work (at %)	63.27 (64.1)	7.2 (8.2)	7.4 (7.5)	6.63 (14.63)	5.9 (1.9)	6.4 (2.1)	1.7 (1.1)	ND	1.5 (0.47)	ND	ND	ND	ND	ND	ND	1658 ± 11
*RENE N5 [®] ²⁰	62.3	7.3	7.9	5.1	4.9	8.1	1.2	ND	3.2	ND	ND	ND	ND	ND	ND	1658 ± 11
RENE N5 [®] ²	63.09	7.0	7.5	6.2	5.0	6.5	1.5	ND	3.0	ND	0.05	ND	0.15	0.01	ND	1593-1723
RENE N5 [®] ⁴	61.80	7.0	8.0	6.2	5.0	7.0	2.0	ND	3.0	ND	ND	ND	ND	ND	ND	-
RENE N5 [®] ²²	63.49	7.01	7.25	6.23	5.05	6.61	1.39	ND	2.71	ND	ND	ND	0.26	ND	ND	1676; 1668; 1648
RENE N5 [®] ²³	60.71	7.48	7.72	6.18	6.38	7.13	1.4	ND	2.85	ND	ND	ND	0.15	ND	ND	-
RENE N5 [®] ²⁴	60.596	7.0	8.0	6.2	5.0	7.0	2.0	1.0	3.0	ND	0.05	ND	0.15	ND	0.004	1660
*RENE 90 [®] ²⁰ , present work (at %)	67.4 (70.08)	8.6 (10.09)	5.2 (5.39)	3.3 (7.46)	7.6 (2.52)	4.9 (1.65)	1.6 (1.02)	1.4 (1.79)	ND	ND	ND	ND	ND	ND	ND	1641 ± 10

^a the compositions of RENE N5[®] and RENE 90[®] superalloys investigated in the present work are also indicated in at %;
ND - non detected.